Resource-Efficient Technologies 3 (2017) 293–302

Contents lists available at ScienceDirect

Resource-Efficient Technologies

journal homepage: www.elsevier.com/locate/reffit

Research paper

Effect of nitrate metal (Ce, Cu, Mn and Co) precursors for the total oxidation of carbon monoxide[☆]

Subhashish Dey[a,*], Ganesh Chandra Dhal[a], Ram Prasad[b], Devendra Mohan[a]

[a] *Department of Civil Engineering, IIT (BHU), Varanasi, India*
[b] *Department of Chemical Engineering and Technology, IIT (BHU), Varanasi, India*

ARTICLE INFO

Article history:
Received 16 November 2016
Revised 27 December 2016
Accepted 30 December 2016
Available online 1 February 2017

Keywords:
Carbon monoxide
Nitrate precursor
Catalyst activity
Reaction temperature
Reactive calcination

ABSTRACT

The ambient temperature carbon monoxide oxidation is one of the important topics in the present scenario. In this paper, we prepared various types of catalysts from the precursors of cobalt nitrate, cerium nitrate, copper nitrate and manganese nitrate for the oxidation of CO. Among the prepared catalysts, the cerium nitrate precursor showed the best performance for CO oxidation at low temperature. The activity of the catalysts was measured in different calcination conditions like stagnant air, flowing air and reactive calcination (4.5% CO in air). The activity test was done in the reactor under the following reaction conditions: 100 mg of catalyst, 2.5% CO in the air and the reaction temperature was increased from ambient to a higher value at which complete oxidation of CO was achieved. The characterization of the catalyst was done by several techniques like XRD, FTIR, SEM-EDX, XPS and BET. The order of activity for different catalysts was as follows: Ce-Oxide > Mn-Oxide > Cu-Oxide > Co-Oxide.

1. Introduction

The oxidation of carbon monoxide (CO) has drawn great attention in recent decades for environmental protection and energy utilization. Automobiles were a good source of CO in the environment, in comparison with a diesel engine, the petrol engine produces more CO in the environment [1]. In the lean burn conditions, the automobiles produce less HC and CO in the exhaust gas in comparison to rich burn conditions [2]. The CO gas damages all livings beings present in the environment. When CO gas enters into the body through the process of respiration, it combines with hemoglobin present in blood cells and is converted into carboxyhemoglobin (CoHb), therefore the oxygen carrying ability in the nerves of the body decreased. Other effects of exposure to CO in the environment on the human body are cardiological problems, neurological damage, coughing, souring, headache, dizziness and nausea etc [3].

A catalytic converter used in an automobiles for emission control purposes converts the toxic pollutants present in exhaust gasses into less toxic pollutants by catalyzing a redox reaction [4]. The noble metals were widely used as a catalyst for a long duration but due to its high price and sulfur poisoning, we have to search for other substitute catalysts like mixed metal oxides and transition metal oxides for CO oxidation purposes [5]. Cobalt oxide was also able to oxidize CO at low temperature due to the presence of lattice oxygen in the catalyst [6,7]. The presence of Co–O bond in Co_3O_4 catalyst was relatively weak and low ΔH was vaporization of O_2 [8–10]. The ceria had a high oxygen storage capacity and high redox properties; therefore, it was making more oxygen available for the oxidation process [11–13]. The size of the catalyst is also an advantage in CO oxidation because the small size particles have a high surface area, which causes an increase in the number of active sites present per unit mass of catalytic material [14,15]. The activation energy of the reaction steps was measured in the FTIR studies for measuring the reaction mechanism [16].

The catalytic oxidation of CO at a low temperature depended upon the various properties of catalysts like crystallite size, catalytic temperature, the mass of catalyst, rate of catalytic reaction and concentration of CO presence in the exhaust gas [17,18]. The catalytic reaction temperature played an important role in the conversion of CO into CO_2 [14]. The MnOx catalyst was prepared from the manganese nitrate precursor and it obtained a high CO conversion efficiency by adding gold in manganese oxide (Au/MnOx) catalyst [19,20].

[☆] Peer review under responsibility of Tomsk Polytechnic University.

[*] Corresponding author. Department of Civil Engineering, IIT (BHU), Varanasi, India. Tel.: +91-9565243424.

E-mail address: subhasdey633@gmail.com (S. Dey).

https://doi.org/10.1016/j.reffit.2016.12.010

The different catalysts had a different properties for the oxidation of CO at a low temperature and the properties of the catalysts were analyzed by different types of characterizations [21]. The catalyst samples were prepared and characterized by means of N_2 sorption, XRD, FTIR, SEM-EDX and XPS analysis. The drying temperature, calcination strategy and the heating rate also have effects on the performance of catalysts for CO oxidation [22]. The catalytic property of the catalysts depends upon the reaction conditions, metal dispersion, types of inorganic supports present and catalyst composition etc [23,24]. The activity of the catalyst was measured by (Nucon) gas chromatography to measure the catalyst activity and product distribution [25].

2. Experimental

2.1. Catalyst preparation

In this paper, we used four different types of nitrate metal precursors for the preparation of catalysts. The precursors used for the preparation of catalysts were cobalt nitrate, cerium nitrate, copper nitrate and manganese nitrate. All the chemicals used for the manufacturing of the catalysts were A.R. grade and they were purchased from the Otto Chemie Company. The nitrate precursors were dried at 120 °C for 12 hr in an oven and calcination at 300 °C for 2 hr in a furnace. The calcination of the precursor was done just before the activity measurement of the catalysts. It was carried out in three ways; first we used stagnant air calcination (SAC) in the absence of air, second was flowing air calcination (FAC) in the presence of air and third was reactive calcination (RC) in the presence of (4.5% of CO in air) at a temperature of 300 °C for 2 h in a compact bench scale of fixed bed tubular reactor [26] (Table 1).

2.2. Characterization

The X-ray diffraction (XRD) measurement of the catalyst was carried out by using Rigaku D/MAX-2400 diffractometer with Cu-Kα radiation at 40 kV and 40 mA. The mean crystallite size (d) of the catalysts was calculated from the line broadening of the most intense reflection using the Scherrer Equation. It provides information about the structure, phase, crystal orientation, lattice parameters, crystallite size, strain and crystal defects etc. The Fourier transform infrared spectroscopy (FTIR) analysis was done by Shimadzu 8400 FTIR spectrometer in the range of 400–4000 cm^{-1}. It provides information about the kind of materials present in a catalyst sample by their peak values. The Scanning electron micrographs (SEM-EDX) produced the topographical image of a catalyst by an electron beam and the image of catalyst was recorded on Zeiss EVO 18 (SEM) instrument. The accelerating voltage used was 15 kV and the applied magnification of the image was 5000×. It provides information about the average aggregate size, crystallinity degree and the microstructures of the catalyst. The X-ray photo electron spectroscopy (XPS) analysis of the catalyst was measured with Amicus spectrometer equipped with Al Kα X-ray radiation at a voltage of 15 kV and a current of 12 mA. It provides information about the surface compositions and chemical states of the different constituent elements present in a catalyst. The Brunauer Emmett Teller Analysis (BET) provides information about the specific surface area, pore size and pore volume of the catalyst. The isotherm was recorded by Micromeritics ASAP 2020 analyzer and the physical adsorption of N_2 at the temperature of liquid nitrogen (−196 °C) with a standard pressure range of 0.05–0.30 P/P_o.

Table 1
The nomenclature used for the catalyst samples in this study was as follows.

Catalyst name	Nomenclature
Cobalt oxide	CoOx
Cerium oxide	CeOx
Copper oxide	CuOx
Manganese oxide	MnOx

2.3. Catalytic activity measurement

After annealing the catalyst bed, it was cooled to room temperature under the same conditions as was used for reactive calcination. The CO oxidation was analyzed by the gas chromatogram to measure the activity of the resulting catalyst.

$$2CO + O_2 \rightarrow 2CO_2 \tag{1}$$

The oxidation of CO was carried out under the following reaction conditions: 100 mg of catalyst with feed gas consisting of a lean mixture of (2.5 vol.% CO in air) and the total flow rate was maintained at 60 mL/min. The air feed into the reactor was made free from moisture and CO_2 by passing through it CaO and KOH pellet drying towers. The catalytic experiment was carried out under the steady state conditions and the reaction temperature was increased from room temperature to 200 °C with a heating rate of 1 °C/min.

To monitor the flow rate of CO and air through the catalyst in the presence of a reactor was done by digital gas flow meters. For controlling the heating temperature of the catalyst present in a reactor was done by a microprocessor based temperature controller. The gaseous products were produced after the oxidation reaction in a reactor was analysis by an online gas chromatogram (Nucon series 5765) equipped with a porapack q-column, FID detector and a methanizer for measuring the concentration of CO and CO_2. The oxidation of CO at any instance was calculated on the basis of concentration CO in the feed and product stream by the following equations:

$$\begin{aligned}(X_{CO}) &= [(C_{CO})_{in} - (C_{CO})_{out}]/[C_{CO}]_{in} \\ &= [(A_{CO})_{in} - (A_{CO})_{out}]/[A_{CO}]_{in} \end{aligned} \tag{2}$$

Where, the concentration of CO was proportional to the area of chromatogram A_{CO}. The overall concentration of CO in the inlet stream was proportional to the area of CO_2 chromatogram.

3. Results and discussions

The characterization of the different catalyst samples prepared in RC conditions was done by the following techniques and the activity of the catalyst for CO oxidation was discussed below.

3.1. Catalyst characterization

The characterization of the catalysts provided information about the morphology, surface area, binding energy, pore volume, pore size, chemical state, material composition and the percentage of different materials presence in a catalyst.

3.1.1. Scanning electron microscopy analysis

The morphology of the prepared catalyst samples in reactive calcination conditions was analyzed by scanning electron microscope. It showed large differences in the surface morphology and other properties of the different prepared catalyst samples (Fig. 1).

The images have shown that the use of different nitrate precursors prepared catalysts makes a large difference in their morphologies. In addition, smaller particle size and good distribution of the active phase present on the catalyst surface cause a significant increase in the effective surface area of the catalyst. As seen in the SEM micrograph, the particles were comprised of more course, course, fine and finest size grains resulting from RC of CoOx, CuOx,

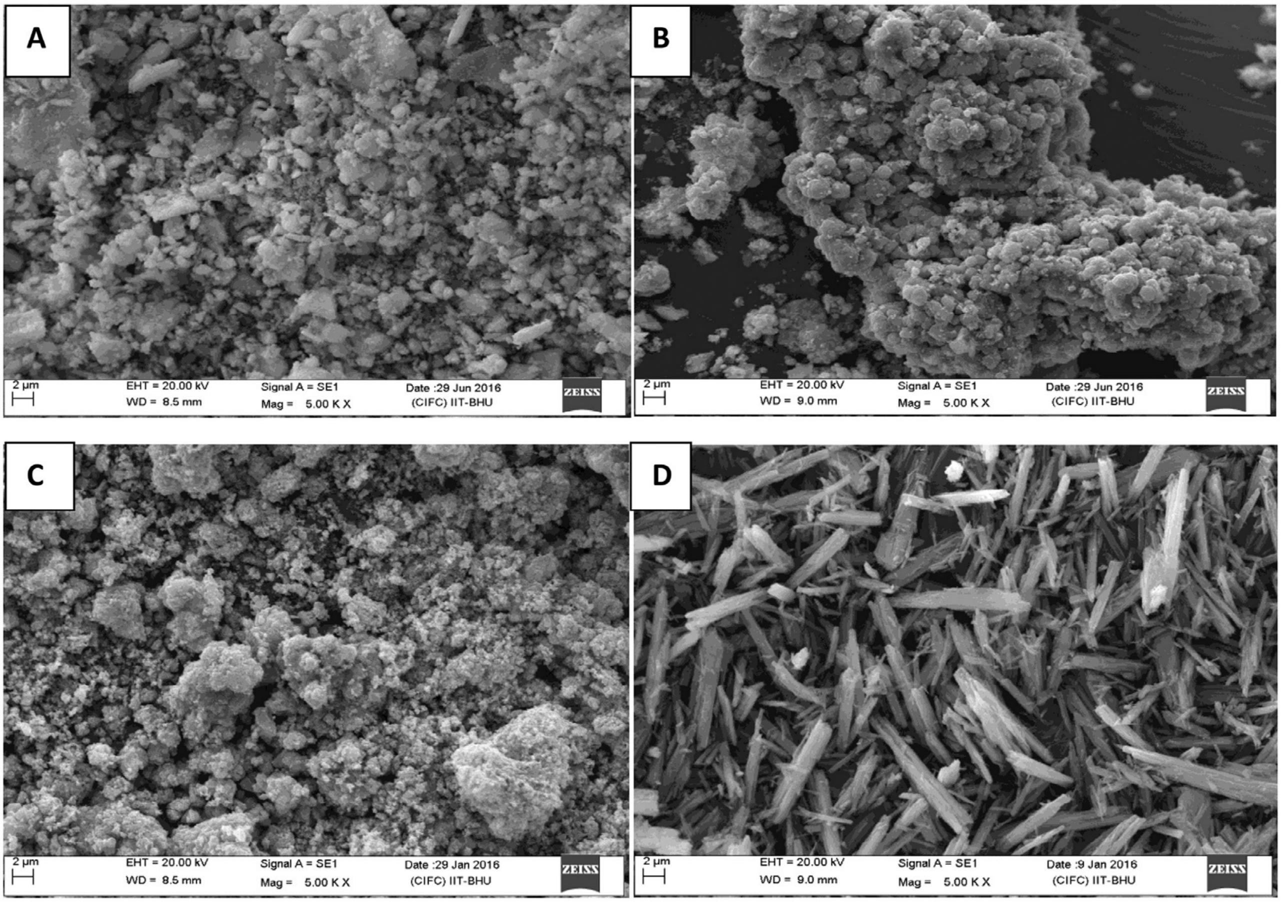

Fig. 1. SEM image of different prepared catalyst samples in RC conditions (A) Ce-Oxide, (B) Mn-Oxide, (C) Cu-Oxide and (D) Co-Oxide.

Table 2
The particle size of different prepared catalyst.

Catalyst	Particle size (μm)
CeOx	0.750
MnOx	0.960
CuOx	1.445
CoOx	2.574

Table 3
The atomic and weight percentage of different catalyst sample by EDX techniques.

Catalyst	Elements atomic (%)		Elements weight (%)	
CeOx	Ce (85.75)	O (14.25)	Ce (84.80)	O (15.20)
MnOx	Mn (72.22)	O (27.78)	Mn (71.85)	O (28.15)
CuOx	Cu (71.11)	O (41.90)	Cu (56.25)	O (43.75)
CoOx	Co (45.35)	O (54.65)	Co (42.65)	O (57.35)

MnOx and CeOx catalysts respectively. The particles present in the CeO_2 and MnO_2 catalysts were smaller in size, less agglomerated and homogeneous as compared to the other catalyst samples. The particle size of the catalyst was also confirmed by the SEM image analysis and it was also observed that particle size of the catalysts increased in the following order: CeOx < MnOx < CuOx < CoOx (Table 2).

The size of granular particles present in a catalyst surfaces was varying between 0.750 and 2.600 μm and it was calculated by "Image J software" with a varying degree of agglomeration. As the particle size of catalysts decreases, more and more CO is dispersed on the surface of the catalyst, which causes an increase in the activity of the catalyst. In the SEM characterization work, we found out that the cerium oxide catalyst have a high surface area as compared to the other three prepared catalyst samples, so that it oxidized more CO into the CO_2 gas. The surface reconstruction behavior of different sizes of particles present in a catalyst surfaces during the prolonged exposure to CO gas. The redox behavior of the ceria materials was attributed to the fast release surface capping oxygen of CeO_2 so that the CO takes this surface capping oxygen and converted into CO_2 gas.

3.1.2. Elemental analysis

It was very clear from the SEM-EDX analysis that all the samples of the catalysts were pure due to the presence of their respective element peaks only (Fig. 2).

After the SEM micrograph was taken, the elemental mapping of different catalyst samples was analyzed to determine the elemental concentration distribution of the catalyst surface. The SEM-EDX was performed on the different spots of the cross-section of the catalyst granules to determine the concentration of different elemental groups present at different locations on the catalyst surfaces. It was very clear from the EDX analysis that the entire catalyst sample was pure as there was no presence of any type of impurities in the catalyst samples.

In Table 3 we can get the relative atomic percentage and weight percentage of different elemental groups present on a surface layer of catalyst. The atomic and weight percentages of oxygen present on the surface layer of catalyst were decreased in the following order: CeOx > MnOx > CuOx > CoOx. The presence of a high concentration of oxygen on a surface layer of a catalyst reduced the

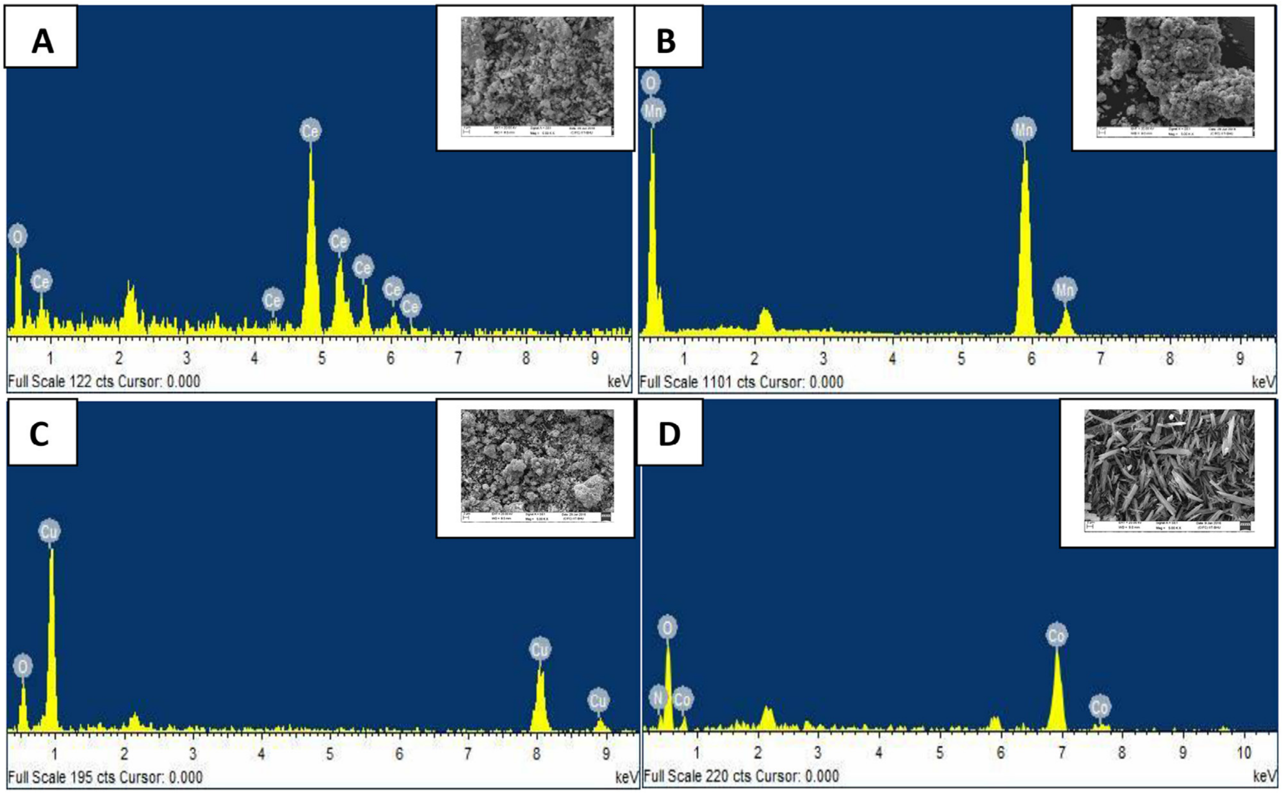

Fig. 2. SEM-EDX image of different catalyst samples prepared in RC conditions (A) Ce-oxide, (B) Mn-oxide, (C) Cu-oxide and (D) Co-oxide.

activity of the catalyst; it was the reason for cobalt oxide catalyst has a poor performance for the oxidation of CO.

It was very clear from the table and figure that the atomic and weight percentage of cerium, manganese and copper elements in a CeOx, MnOx and CuOx catalyst was higher than oxygen but in a CoOx catalyst the percentage level of cobalt element present in a surface layer of catalyst was less than oxygen. The increasing of oxygen concentration in a surface layer catalyst, therefore, the activity of the catalyst was decreased. Due to the high oxygen deficiency present in the cerium oxide (CeOx) catalyst, therefore the activity of the catalyst was increased. The high level of oxygen deficiency was created the high density of active sites present on a catalyst surface. It was also confirmed that the presence of pure oxides phase on the catalyst surfaces was also a good harmony with the XRD and FTIR results also.

Table 4
The crystalline size of the catalyst.

Catalyst	Crystalline size (nm)
CeOx	7.625
MnOx	21.19
CuOx	28.19
CoOx	32.76

Table 5
The comparison study of crystalline size and particle size of different catalyst.

Catalyst	Crystalline size (nm)	Particle size (μm)
CeOx	7.625	0.750
MnOx	21.19	0.960
CuOx	28.19	1.445
CoOx	32.76	2.574

3.1.3. X-ray diffractogram of the catalysts

The XRD pattern of the different catalyst samples of (CeOx, CuOx, MnOx and CoOx) calcined in RC conditions was shown in Fig. 3. The XRD study of the catalyst samples was carried out to identify the crystalline size and coordinate dimensions present on the surface layer of catalysts.

The phase analysis of different prepared catalyst samples was done by the XRD studies. In the CeOx catalyst their diffraction peak at 2-Theta (2θ) was 56.43 and their corresponding lattice plane (h k l) value was (3 1 1) at the JCPDS reference no. (81-0792). The structure was face-centered cubic CeO_2 phase and crystallite size of the catalyst was 7.625 nm. In the MnOx catalyst their diffraction peak at 2-Theta (2θ) was 38.95 and their corresponding lattice plane (h k l) value was (2 1 1) at the JCPDS reference no. (89-2545). The structure was end centered; monoclinic MnO_2 phase and crystallite size of the catalyst was 21.19 nm.

In the CuOx catalyst their diffraction peak at 2-Theta (2θ) was 35.55 and their corresponding lattice plane (h k l) value was (1 1 1) at the JCPDS reference no. (89-2530). The structure was end centered; monoclinic CuO_2 phase and crystallite size of the catalyst was 28.19 nm. In the CoOx catalyst their diffraction peak at 2θ was 55.86 and their corresponding lattice plane was (4 2 2). The structure was face-centered cubic Co_3O_4 phase and crystallite size of the catalyst was 32.76 nm (Table 4).

The crystalline size of the catalyst increased in the following order: CoOx > CuOx > MnOx > CeOx, which matches with SEM image analysis of the catalysts. The experimental result proved that the lower particle size of CeOx catalyst was highly active for oxidation of CO at a low temperature. The activation or deactivation periods on the catalytic reaction and the loss or gain of catalytic activity on the reaction may be related to the appearance or loss of specific bulk phases. The comparison study between crystallite and particle sizes of different prepared catalyst samples was shown in Table 5.

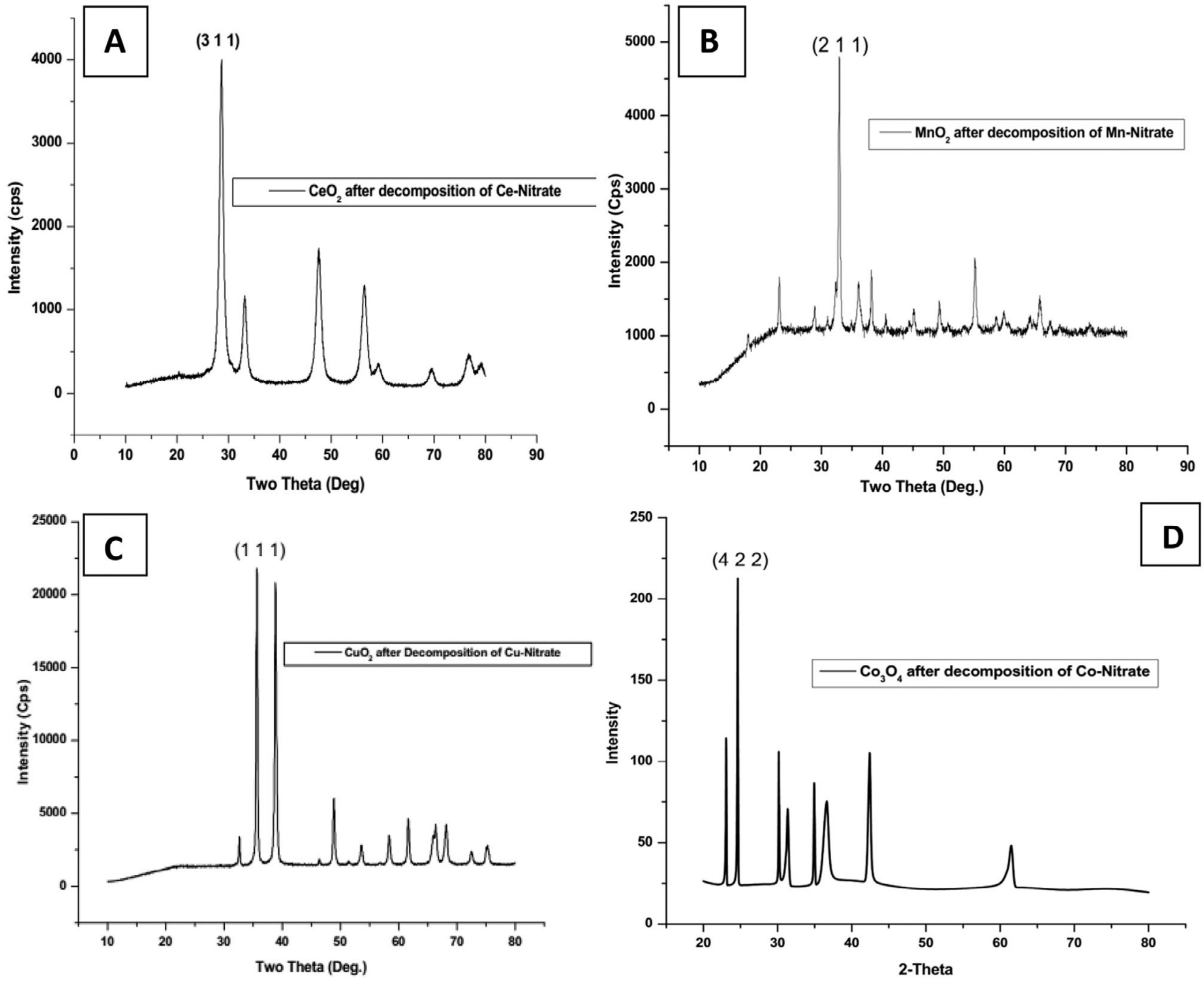

Fig. 3. XRD analysis of different prepared catalyst samples in RC conditions (A) CeOx, (B) MnOx, (C) CuOx and (D) CoOx.

The crystallite size of catalysts should be obtained from XRD analysis and particle size of catalysts should be obtained from SEM analysis and it is increased in the following order: CoOx > CuOx > MnOx > CeOx. After the SEM and XRD analyses we can get that the crystalline size and particle size of the catalyst, which follow the same order.

3.1.4. *Fourier transforms infrared spectroscopy (FTIR)*

The FTIR transmission spectrum of the different prepared catalyst samples was shown in Fig. 4. The FTIR peaks analyses were obtained in the invested regions between (4000–400 cm^{-1}). The entire absorption spectra of different peaks indicate the presence of different elemental groups in the catalyst samples. All the catalyst samples were prepared in RC conditions before application in different characterization work. Four peaks were obtained in the FTIR analysis of the CeOx catalyst in the transmittance conditions. The IR band (1510 cm^{-1} and 1330 cm^{-1}) shows the presence of $CO_3{}^{2-}$ group and (2720 cm^{-1} and 1820 cm^{-1}) shows the presence CeOx group respectively. In the MnOx catalyst at the transmittance conditions, eight peaks were obtained. The IR band (3590 cm^{-1}) shows the presence of –OH group, (3040 cm^{-1} and 2350 cm^{-1}) shows the presence of COO group, (1640 cm^{-1} and 1530 cm^{-1}) shows the presence of MnO_2 group and (1250 cm^{-1} and 525 cm^{-1}) shows the presence of $CO_3{}^{2-}$ group respectively.

In the CuOx catalyst at the transmittance conditions, six peaks were obtained. The IR band (3529 cm^{-1}) shows the presence of –OH group, (2994 cm^{-1}) shows the presence of –NH group, (1699 cm^{-1}) shows the presence of C=O group, (1388 cm^{-1}) shows $CO_3{}^{2-}$ group and (615 cm^{-1} and 577 cm^{-1}) shows the presence of CuO_2 group respectively.

In the CoOx catalyst at the transmittance conditions, ten peaks were obtained. The IR band (3710 cm^{-1} and 3380 cm^{-1}) shows the presence of O–H group, (663 cm^{-1} and 2870 cm^{-1}) shows the presence of CoO_x group, (2750 cm^{-1}) shows the presence of Cobalt Carbonyl group, (1290 cm^{-1} and 1440 cm^{-1}) shows the presence of Co_3O_4 group, the weak band (1110 cm^{-1}) shows the presence of COO group and (710 cm^{-1} and 548 cm^{-1}) shows the presence of cobalt oxide species respectively. After the FTIR analysis, we found out that the CeOx catalyst was highly pure as compared to the other three prepared catalyst samples in RC conditions. There will be some impurities like carbonate group and hydroxyl group present in a CuOx and CoOx catalyst sample. The intensity of impurities present in a catalyst sample was analyzed by the FTIR study and it was decreased in the following order: CoOx > CuOx > MnOx > CeOx.

3.1.5. *XPS analysis*

With the help of XPS analysis, we can get the surface valence state, binding energy and the chemical state of different

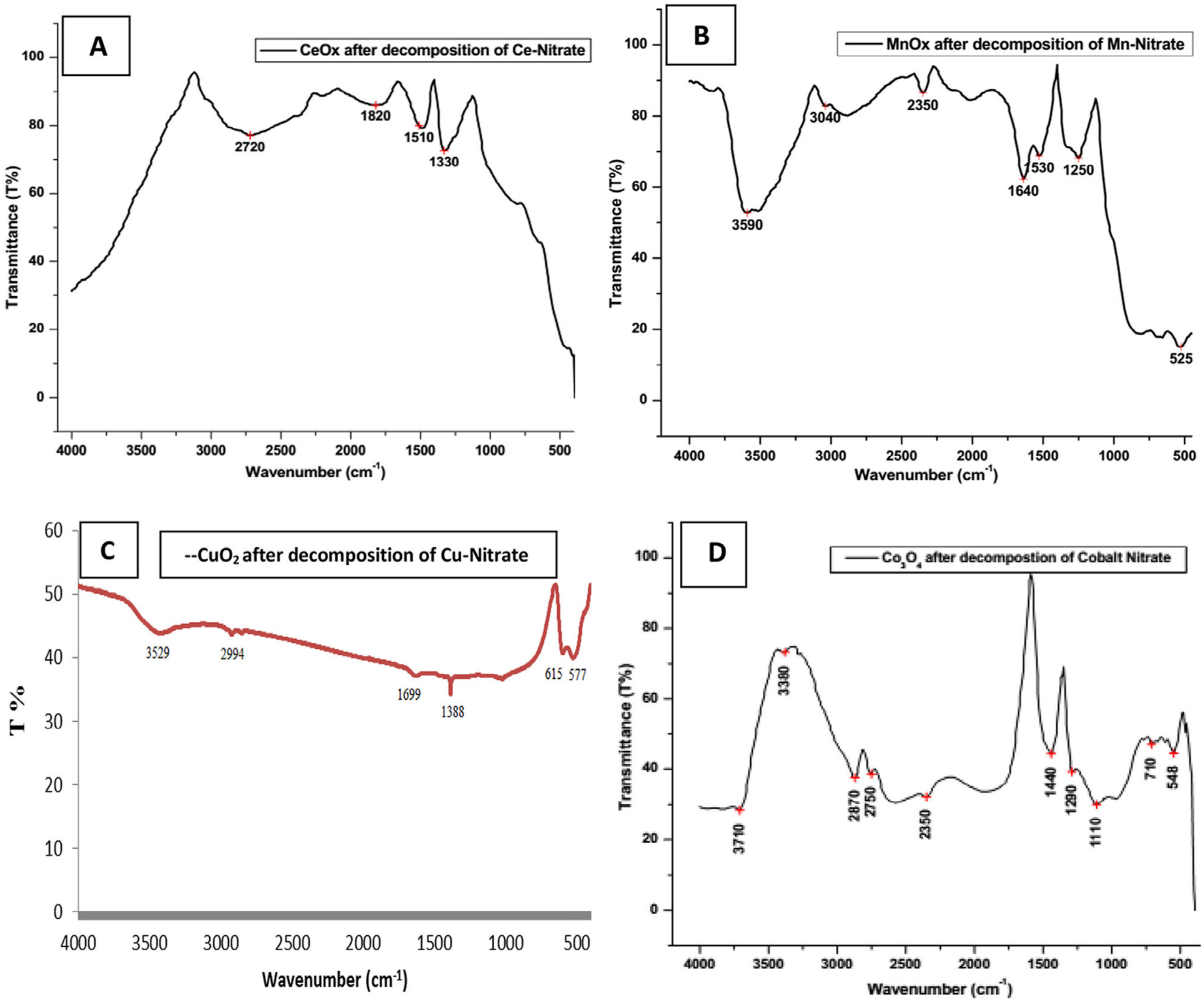

Fig. 4. FTIR analysis of different prepared catalyst samples in RC conditions (A) CeOx, (B) MnOx, (C) CuOx and (D) CoOx.

Table 6
The chemical state and binding energy of the prepared catalyst samples in RC conditions.

Catalyst	Chemical state of elements		Binding energy of elements	
CeOx	Ce (III) oxide	Organic C–O	Ce (879.36)	O (533.20)
MnOx	MnO_2	Organic C–O	Mn (656.54)	O (534.86)
CuOx	Cu (II) oxide	Organic C=O	Cu (628.29)	O (535.46)
CoOx	Co_3O_4	Organic C=O	Co (582.79)	O (532.80)

elemental groups present on a catalyst surface. All the catalyst samples were prepared in RC conditions and the higher binding energy was preferably for the CO oxidation reaction. Table 6 shows the binding energy and the chemical state of different elemental groups present in a catalyst surface.

According to the latest research the bands of 278 and 313 nm for pure CeO_2 can be ascribed to the overlapping of the $Ce^{4+} \leftarrow O^{2-}$ charge transfer and inter brands transaction respectively. The catalytic activity of the CeO_2 base materials increases proportionally with the band gaps. All the binding energies (BE) were referenced to the adventitious C(1s) line at 284.6 eV ($1\ eV = 1.602 \times 10^{-19}$ J). The Ce($3d^{5/2}$) peak was the composition of two corresponding Ce^{3+} and Ce^{4+} species, with the prevalence of the former species.

From the table, it is shown that the Ce ions present in a CeOx catalyst was Ce (III) oxide form, Mn ions present in a MnOx catalyst was MnO_2 form, Cu ions present in a CuOx catalyst was Cu (II) oxide form and Co ions present in a CoOx catalyst was Co_3O_4 form.

The binding energy of Ce(3d), Mn(2p), Cu(2p) and Co(2p) elements present in a CeOx, MnOx, CuOx and CoOx catalyst was 879.36 eV, 656.54 eV, 628.29 eV and 582.79 eV respectively. From the table and figure it was clear that the binding energy presence is the highest in CeOx catalyst and lowest in CoOx catalyst. The major peaks of the Ce(3d) were deconvoluted into three peaks centered at 892.320 eV, 879.372 eV and 886.308 eV presences respectively (Fig. 5).

Although, it can be proposed that the highest binding energy was preferably for the CO oxidation reactions. The increases of Ce ions concentration in the CeOx catalyst was helpful to the migration of oxygen from bulk to the catalyst surface, which can promote the activation and transportation of active oxygen species on the surface of catalyst. The binding energy of oxygen O (1s) spectra was illustrated in Fig. 6. In the XPS analysis there were two diverse types of oxygen species present in all catalyst samples. First was known as chemisorbed oxygen (O_a) which had a binding energy of (529.2–530 eV) and second was known as lattice oxygen (O_l) which had a binding energy of (531.3–532.2 eV) respectively.

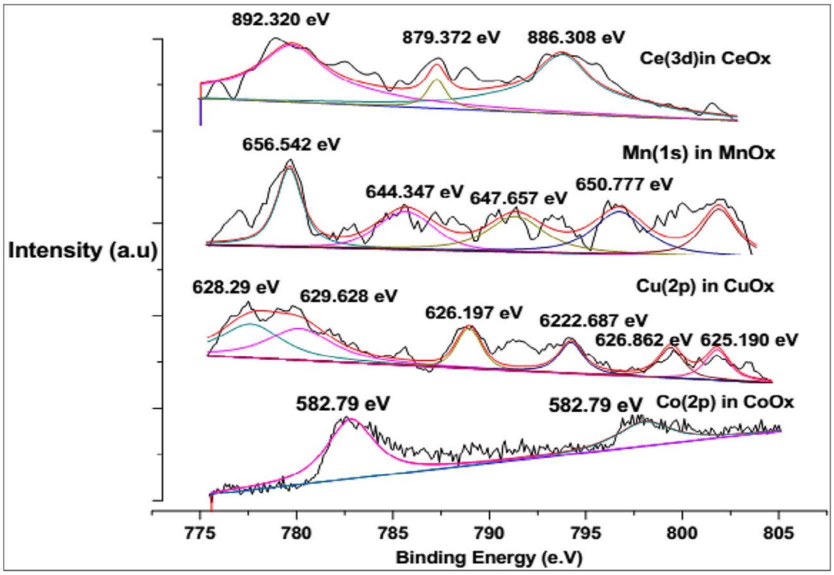

Fig. 5. XPS analysis of the catalyst samples prepared in RC conditions.

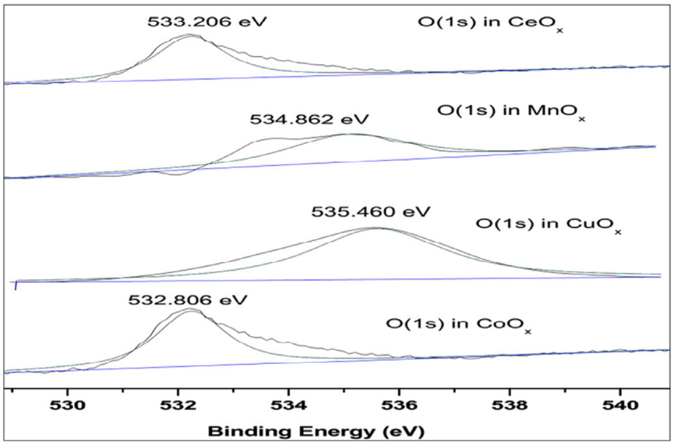

Fig. 6. XPS analysis of oxygen O (1s) species present on a catalyst surface.

In our present study the oxygen with binding energy of (532.80 eV–535.46 eV) could be assigned and it was well known that the high amount of surface chemisorbed oxygen was enhancing the activity of the resulting catalyst. The oxygen peaks spectra present in a CeOx catalyst was much broader and more intensive than the other three prepared catalyst samples. Therefore, it suggests that the highest binding energy of CeOx catalyst was more preferable for the selective catalytic activity reaction.

3.1.6. BET surface area

The surface area of different prepared catalyst samples like CeOx, MnOx, CuOx and CoOx in RC conditions were 48.03 m^2/g, 35.90 m^2/g, 31.84 m^2/g and 24.60 m^2/g respectively. The pore volume and pore size of the CeOx catalyst was slightly higher than the other three prepared catalyst samples and it was shown in Table 7.

The textural properties like surface area, pore volume and pore size of the catalysts were more preferable for the CO oxidation reactions. The larger number pores present on a catalyst surface means a larger number of CO molecules trapped and they have to show the better catalytic activity at low temperature. The specific surface area of the catalysts was measured by BET analysis and it matched with the SEM and XRD results. The cerium oxide (CeOx) and manganese oxide (MnOx) catalyst surface areas and pore volumes were so high so that it was most active for CO oxidation reaction at a low temperature, but it was several times deactivated by trace amount of moisture present in a catalyst (Fig. 7).

Table 7
The textural properties of the different catalyst sample in RC conditions.

Catalyst	Surface area (m^2/g)	Pore volume (cm^3/g)	Average pore size (Å)
CeOx	48.03	0.470	58.06
MnOx	35.90	0.430	46.05
CuOx	31.84	0.380	37.36
CoOx	24.60	0.310	25.60

3.2. Catalyst performance and activity measurement

The catalyst activity test was carried out to evaluate the effectiveness of different prepared catalyst samples (CeOx, MnOx, CuOx and CoOx) as a function of temperature. The activity of the catalysts was evaluated in a different calcination conditions like stagnant air (SAC), flowing air (FAC) and reactive calcination (RC) conditions into the laboratory. The light-off characteristics was used to measure the activity of the resulting catalysts with the increasing of temperature. The characteristic temperature T_{10}, T_{50} and T_{100} represents the initiation of the oxidation, half conversion and full conversion of CO respectively.

3.2.1. Stagnant air calcination conditions

The final treatment (calcination) of the catalyst precursors to controls the final distribution of active metals. In the stagnant air calcination conditions, the activity of the resulting catalysts was initiated near around at the room temperature. The decomposition behavior of the precursors under the heating conditions was observed to be differing significantly from that under the continuous heating. The oxidation of CO was just initiated in stagnant air calcination conditions at 25 °C, 30 °C, 35 °C and 35 °C over the CeOx, MnOx, CuOx and CoOx catalyst respectively (Fig. 8).

The half conversion of CO was 100 °C for CeOx catalyst, which was less by 10 °C, 35 °C and 65 °C over the MnOx, CuOx and CoOx catalyst respectively. It was clear from the table and figure that the activity of the resulting catalysts lies between 30 °C and 280 °C temperature. The rising temperature enlarged the specific surface

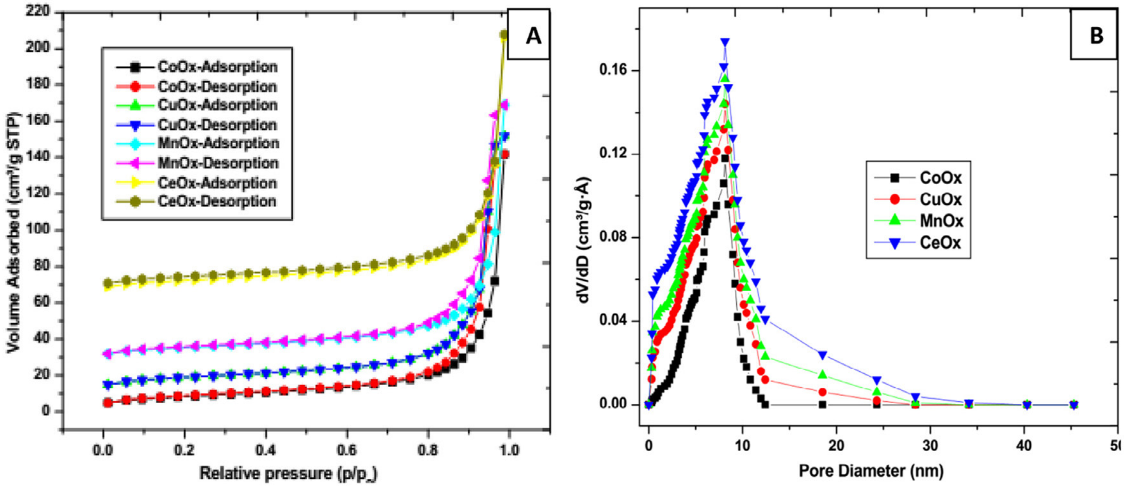

Fig. 7. The textural properties (A) N_2 adsorption-desorption isotherms and (B) Pore size distributions curves.

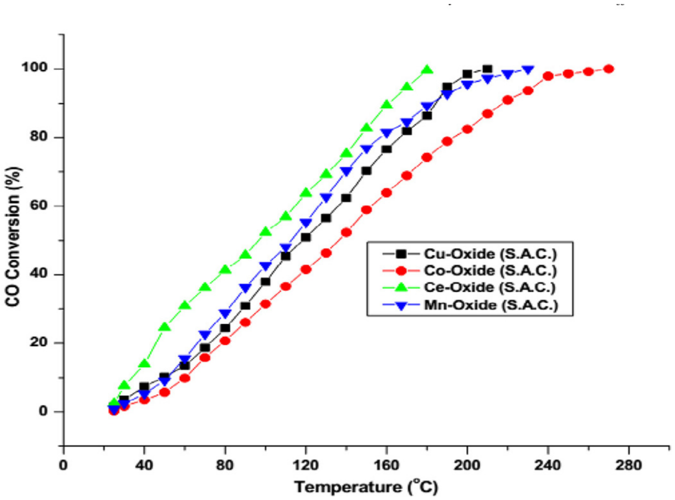

Fig. 8. The activity test of different prepared catalysts in SAC conditions.

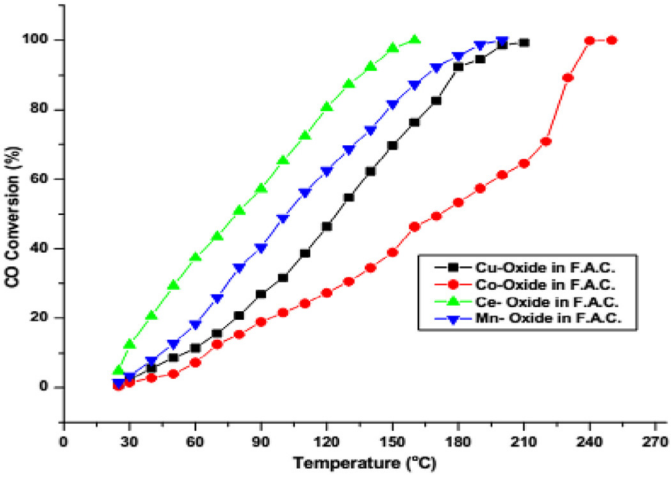

Fig. 9. The activity test of different prepared catalysts in FAC conditions.

area and pore volume of the catalyst therefore the activity of the catalyst was increased (Table 8).

The complete oxidation of CO over CoOx catalyst was observed at 85 °C higher than that over CeOx catalyst. The total oxidation temperature of CeOx catalyst was 190 °C, which was less by 20 °C and 35 °C over the MnOx and CuOx catalyst respectively and the reaction was exothermic in nature. It was very clear from the table and figure that the CeOx catalyst was highly active for CO oxidation at a low temperature as compared to the other three prepared catalyst samples and the order of activity of different prepared catalyst samples in stagnant air calcination conditions was as follows: CeOx > MnOx > CuOx > CoOx. The extraordinary performance of the CeOx catalyst was highly active for the completely oxidation of CO at low temperature.

3.2.2. Flowing air calcination conditions

In the flowing air calcination conditions, a fresh catalyst was used to measure the activity of the resulting catalysts at each temperature. In the initial conditions, a very slow exothermic reaction for CO oxidation was going on over the catalyst, it causes a rise in local temperature. The rise in local temperature will reduce the decomposition of the precursor. The copper nitrate and manganese nitrate was most widely used as precursors in the preparation of different types of CuMnOx catalyst. The individual property of copper nitrate and manganese nitrate precursors has also an effect on the preparation of resulting catalyst. Fig. 9 and Table 9 show the activity of different prepared catalyst samples in flowing air calcination conditions.

The oxidation of CO was just initiated in flowing air calcination conditions at 25 °C, 28 °C, 30 °C and 35 °C over the CeOx, MnOx,

Table 8
The light of temperature of the catalysts for CO oxidation in SAC conditions.

Catalyst	T_{10}	T_{50}	T_{100}
CeOx	25 °C	100 °C	190 °C
MnOx	30 °C	110 °C	210 °C
CuOx	35 °C	135 °C	225 °C
CoOx	35 °C	165 °C	275 °C

Table 9
The light of temperature of the catalysts for CO oxidation in FAC conditions.

Catalyst	T_{10}	T_{50}	T_{100}
CeOx	25 °C	85 °C	160 °C
MnOx	28 °C	100 °C	175 °C
CuOx	30 °C	130 °C	190 °C
CoOx	35 °C	155 °C	255 °C

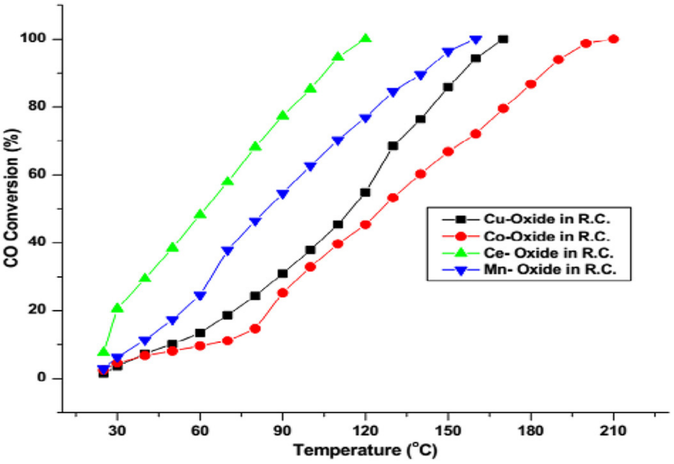

Fig. 10. The activity test of different prepared catalysts in RC conditions.

CuOx and CoOx catalysts respectively and the complete oxidation of CO by CeOx catalyst was 160 °C temperature, which was less by 15 °C, 30 °C and 95 °C over than that of MnOx, CuOx and CoOx catalysts respectively. The complete CO oxidation process over the different prepared catalyst samples in flowing air calcination conditions was between the reaction temperatures of 30 °C and 270 °C. The calcination conditions change the arrangement of the surface molecules to some degree and affects the metal-support interactions. From the table and figure, we have to finalize that the CeOx catalyst was shows highest activity for CO oxidation at a low temperature as compared to the other three prepared catalyst samples. There was a large gap between the CO oxidation over the CeOx catalyst compared with other three prepared catalyst samples in flowing air calcination conditions as shown in Fig. 9.

In comparison between the stagnant air and flowing air calcination conditions, we have to find out that the flowing air calcination conditions were showed the best activity for CO oxidation at a lower temperature as compared to the stagnant air calcination conditions. The order of activity of different prepared catalyst samples in flowing air calcination conditions was as follows: CeOx > MnOx > CuOx > CoOx. The improved catalytic activity of the CeOx catalyst can be ascribed to the unique structural, textural chacateristics and the smallest crystalline size. The rate of CO oxidation was increased with time and flattened at the end. This might be due to the synergistic effects of exothermic oxidation, decomposition and redox surface reaction of the catalyst surfaces.

3.2.3. Reactive calcination conditions

The reactive calcination of different prepared catalyst samples was carried out by passing a CO-Air mixture over the precursors at 160 °C for 20 min and 300 °C for 30 min for total decomposition of the catalyst. In the Fig. 10, we have to scene that the comparison study of CO oxidation by various types of catalysts prepared in RC conditions. The extra ordinary performance of the resulting catalysts was achieved for full conversion of CO at lower temperature in RC conditions. The novelty of the catalysts produced by RC conditions was matches with their different characterization results.

Table 10
The light of temperatures of the catalysts for CO oxidation in RC conditions.

Catalyst	T_{10}	T_{50}	T_{100}
CeOx	25 °C	60 °C	120 °C
MnOx	25 °C	80 °C	160 °C
CuOx	25 °C	120 °C	165 °C
CoOx	30 °C	150 °C	215 °C

The oxidation of CO was initiated in reactive calcination conditions at 25 °C, 25 °C, 25 °C and 35 °C over the CeOx, MnOx, CuOx and CoOx catalyst respectively. The preparation of the catalysts for the oxidation of CO varied between 25 °C and 215 °C temperature in RC conditions. The total oxidation temperature of CO was 120 °C for CeOx catalyst, which was less by 40 °C, 45 °C and 95 °C than that of MnOx, CuOx and CoOx catalysts respectively. Thus, it was apparent from the table and figure that the catalyst samples prepared by the RC conditions were more active during CO oxidation at low temperatures as compared to the stagnant air or flowing air calcination conditions. A comparison study of the light-off temperatures of all the catalyst samples prepared by RC conditions was given below in the Table 10.

The light-off temperature also showed that the RC conditions prepared catalysts were more active during CO oxidation at low temperatures as compared to the stagnant air or flowing air calcination conditions prepared catalysts. The activity order of the catalysts for CO oxidation was in accordance with their characterization by XRD, SEM-EDX, FTIR, XPS and BET analyses as follows: CeOx > MnOx > CuOx > CoOx. The CeOx catalysts have the high surface area so that more CO easily dispersed on the surface side of catalysts.

3.2.4. The comparison study of different prepared catalysts

The comparison study of different prepared catalyst samples in different calcination conditions was shown in Table 11. The RC condition increased the number of texture pores present in catalyst surfaces, which is favorable during the adsorption of the reactants and desorption of the products and the facilitation of the oxidation process. The RC condition improved the unique structures present in catalyst surfaces like textural characteristics, crystalline size, surface area, etc. The CO_2 gas can be formed during the irreversible desorption of CO, thus CO_2 adsorption peaks increase due to the irreversible desorption of CO.

The results demonstrated that the catalyst prepared by RC conditions was highly active for completely oxidation of CO at a low temperature in the range of 120 °C to 220 °C. The best catalyst activity was also exhibited by both their excellent long term stability and good cycling activity due to the presence of their crystalline nature. The presence of crystalline nature of the catalyst it will be makes an ideal catalyst for low temperature CO oxidation. The catalytic reaction was also faster at elevated temperatures because CO was desorbed and it was significantly allowed for the dissociative of O_2 adsorption. The oxidation reaction was also associated with the cluster size of the catalyst, catalyst concentration and oxygen bonding moieties present on a catalyst surface.

In the CO oxidation process, there were two steps of reaction mechanism; in the first stage CO reacts on the catalyst surface to form an OCO and in the second stage of dissociation to form CO_2 in the gas phase. The presence of partially reduced phase in RC conditions prepared catalysts to provide more oxygen deficient defective structures which create the highest density of active sites for total conversion of CO. The experimental results has shown that the calcination strategy of the precursors has greatly influenced the activity of the resulting catalyst. The order of activity in different calcination conditions of the prepared catalyst was as follows: RC > FAC > SAC.

A small change in a lattice constant was highly affecting the binding energy of surface species presence in a catalyst surface. The reaction rate for CO oxidation highly depends upon the number of active sites, exposed facets and the step edge presence on the surface of the catalyst. In the activity test it was seen that the CeOx catalyst prepared by RC conditions, shows the best result for the total oxidation of CO at a low-temperature due to the presence of high surface area (48.03 m^2/g), high pore size (58.06 Å), small

Table 11
The activity test of different prepared catalysts in the different calcination conditions.

Calcination strategy	CeOx catalyst			MnOx catalyst			CuOx catalyst			CoOx catalyst		
	T_i	T_i	T_i	T_i	T_{50}	T_{100}	T_i	T_{50}	T_{100}	T_i	T_{50}	T_{100}
RC	25 °C	60 °C	120 °C	25 °C	80 °C	160 °C	25 °C	120 °C	165 °C	30 °C	150 °C	215 °C
FAC	25 °C	85 °C	160 °C	28 °C	100 °C	175 °C	30 °C	130 °C	190 °C	35 °C	155 °C	255 °C
SAC	25 °C	100 °C	190 °C	30 °C	110 °C	210 °C	35 °C	135 °C	225 °C	35 °C	165 °C	275 °C

crystalline size (7.625 nm) and the high binding energy (879.36 eV) in a catalyst.

4. Conclusions

The preparation conditions, calcination strategies and aging time have a great influence on the activity of the resulting catalyst. From the results and discussions, we have to conclude that the RC route was the most appropriated calcination strategy for the production of a highly active catalyst for CO oxidation at a low temperature. The calcination order with respect to the performance of the catalyst for CO oxidation was as follows: Reactive calcination > Flowing air calcination > Stagnant air calcination. In the activity test we found out that the CeOx catalyst prepared by RC conditions was showed the best catalytic activity for CO oxidation at a low temperature (120 °C).

The performance of the catalysts was in accordance with their characterization, therefore it was suggested that the oxygen-deficient defective structure which produces a high density of surface area. Due to the presence of a high density of surface area the active sites present on a catalyst surface increased. The activation energy barrier present in the CO_2 gas phase increased as the size of the particles increased. The order of activity for different prepared catalyst samples in different calcination conditions was as follows: Ce-Oxide > Mn-Oxide > Cu-Oxide > Co-Oxide. Therefore it was suggested that the smallest particle size of CeOx catalyst was highly active for CO oxidation at low temperature as compared to the other prepared catalyst samples.

References

[1] G.S. Cholakov, Control of exhaust emissions from internal combustion engine vehicles, Pollut. Control Technol 3 (2000) 1–8.

[2] P. Gélin, L. Urfels, M. Primet, E. Tena, Complete oxidation of methane at low temperature over Pt and Pd catalysts for the abatement of lean-burn natural gas fuelled vehicles emissions: influence of water and sulphur containing compounds, Catal. Today 83 (2003) 45–57.

[3] K. Rajiah, E.M. Mathew, Clinical manifestation, effects, diagnosis, monitoring of carbon monoxide poisoning and toxicity, Afr. J. Pharm. Pharmacol 5 (2011) 259–264.

[4] A. Ghaffari, A.H. Shamekhi, A. Saki, E. Kamrani, Adaptive fuzzy control for air–fuel ratio of automobile spark ignition engine, World Acad. Sci. Eng. Technol 48 (2008) 284–292.

[5] C. Tang, C. Kuo, M. Kuo, C. Wang, S. Chien, Influence of pretreatment conditions on low-temperature carbon monoxide oxidation over CeO_2/Co_3O_4 catalysts, Appl. Catal. A Gen 309 (2006) 37–43.

[6] A. Alvarez, S. Ivanova, M.A. Centeno, J.A. Odriozola, Sub-ambient CO oxidation over mesoporous Co_3O_4: effect of morphology on its reduction behavior and catalytic performance, Appl. Catal. A Gen 431 (2012) 9–17.

[7] M.J. Pollard, B.A. Weinstock, T.E. Bitterwolf, P.R. Griffiths, A.P. Newbery, J.B. Paine, A mechanistic study of the low temperature conversion of carbon monoxide to carbon dioxide over a cobalt oxide catalyst, J. Catal 254 (2008) 218–225.

[8] F. Balikci, C. Guldur, Characterization and CO oxidation activity studies of Co based catalyst, Turk. J. Chem 31 (2007) 465–471.

[9] A. Biabani-Ravandi, M. Rezaei, Z. Fattah, Study of Fe-Co mixed metal oxide nanoparticles in the catalytic low temperature CO oxidation, Process Saf. Environ. Prot 91 (2013) 489–494.

[10] J. Cao, G. Li, Y. Wang, G. Sun, X. Wang, B. Hari, et al., Mesoporous Co-Fe-O nanocatalysts: preparation, characterization and catalytic carbon monoxide oxidation, J. Environ. Chem. Eng 2 (2014) 477–483.

[11] D.A.H. Cunningham, T. Kobayashi, N. Kamijo, M. Haruta, Influence of dry operating conditions: observation of oscillations and low temperature CO oxidation over Co_3O_4 and Au/Co_3O_4 catalysts, Catal. Lett 25 (1994) 257–264.

[12] Z. Shanghon, B. Xue, W. Xiaoyan, Y. Wenguo, L. Yuan, Valence state of active copper in $CuOx/CeO_2$ catalysts for CO oxidation, J. Rare Earths 240 (2006) 177–181.

[13] P.V. Snytnikov, M.M. Popova, Y. Men, E.V. Rebrov, G. Kolb, V. Hessel, et al., Preferential CO oxidation over a copper–cerium oxide catalyst in a micro channel reactor, Appl. Catal. A Gen 350 (2008) 53–62.

[14] K.S. Abdel Halim, M.H. Khedr, M.I. Nasr, A.M. El-Mansy, Factors affecting CO oxidation over nanosized Fe_2O_3, Mater. Res. Bull 42 (2007) 731–741.

[15] C. Hu, Z. Gao, X. Yang, Facile synthesis of single crystalline α-Fe_2O_3 ellipsoidal nanoparticles and its catalytic performance for removal of carbon monoxide, Mater. Chem. Phys 104 (2007) 429–433.

[16] X. Zheng, S. Wang, S. Wang, S. Zhang, W. Huang, S. Wu, Copper oxide catalysts supported on ceria for low temperature CO oxidation, Catal. Commun 5 (2004) 729–732.

[17] P.W. Park, J.S. Ledford, The influence of surface structure on the catalytic activity of alumina supported copper oxide catalysts oxidation of carbon monoxide and methane, Appl. Catal. B 15 (1998) 221–231.

[18] V.A. Sadykov, S.F. Tikhov, N.N. Bulgakov, A.P. Gerasev, Catalytic oxidation of CO on CuOx revisited: impact of the surface state on the apparent kinetic parameters, Catal. Today 144 (2009) 324–333.

[19] S. Lee, A. Gavriilidis, Q.A. Pankhurst, A. Kyek, F.E. Wagner, P.C.L. Wong, et al., Effect of drying conditions of Au-Mn co-precipitates for low temperature CO oxidation, J. Catal 200 (2001) 298–308.

[20] M. Roy, S. Basak, M.K. Naskar, Bi-template assisted synthesis of mesoporous manganese oxide nanostructures: tuning properties for efficient CO oxidation, Phys. Chem. Chem. Phys 18 (2016) 5253–5263.

[21] L.Q. Qwabe, H.B. Friedrich, S. Singh, Preferential oxidation of CO in a hydrogen rich feed stream using Co-Fe mixed metal oxide catalysts prepared from hydrotalcite precursors, J. Mol. Catal. A Chem, 404 (2015) 167–177.

[22] G.G. Xia, Y.G. Yin, W.S. Willis, J.Y. Wang, S.L. Suib, Efficient stable catalysts for low temperature carbon monoxide oxidation, J. Catal 185 (1999) 91–105.

[23] M. Skaf, S. Aouad, S. Hany, R. Cousin, E. Abi-Aad, A. Aboukaïs, Physicochemical characterization and catalytic performance of 10% Ag/CeO_2 catalysts prepared by impregnation and deposition–precipitation, J. Catal 320 (2014) 137–146.

[24] P. Bose, S. Ghosh, S. Basak, M.K. Naskar, A facile synthesis of mesoporous NiO nanosheets and their application in CO oxidation, J. Asian Ceram. Soc 4 (2016) 1–5.

[25] S. Rojanapipatkul, J.G. Goodwin, P. Praserthdam, B. Jongsomjit, Effect of cobalt precursors on properties of $Co/CoAl_2O_4$ catalysts synthesized by solvothermal method, Eng. J. 16 (2012) 1–4.

[26] R. Prasad, P. Singh, A novel route of single step reactive calcinations of copper salts far below their decomposition temperatures for synthesis of highly active catalysts, Catal. Sci. Technol 3 (2013) 3326–3334.